ADVANCES IN ATMOSPHERIC SCIENCES, VOL. 24, NO. 1, 2007, 82–88

Comparison Between GAMIL, and CAM2 on Interannual Variability Simulation

YANG Junli*[1,2] (杨军丽), WANG Bin[1] (王 斌), GUO Yufu[1] (郭裕福), WAN Hui[1,2] (万 慧), and JI Zhongzhen[1] (季仲贞)

[1] *State Key Laboratory of Numerical Modeling for Atmospheric Sciences and Geophysical Fluid Dynamics, Institute of Atmospheric Physics, Chinese Academy of Sciences, Beijing* 100029

[2] *Graduate University of the Chinese Academy of Sciences, Beijing* 100039

(Received 15 August 2005; revised 13 June 2006)

ABSTRACT

Recently, a new atmospheric general circulation model (GAMIL: Grid-point Atmospheric Model of IAP LASG) has been developed at the Institute of Atmospheric Physics (IAP), Chinese Academy of Sciences (CAS), which is based on the Community Atmospheric Model Version 2 (CAM2) of the National Center for Atmospheric Research (NCAR). Since the two models have the same physical processes but different dynamical cores, the interannual variability simulation performances of the two models are compared. The ensemble approach is used to reduce model internal variability.

In general, the simulation performances of the two models are similar. Both models have good performance in simulating total space-time variability and the Southern Oscillation Index. GAMIL performs better in the Eastern Asian winter circulation simulation than CAM2, and the model internal variability of GAMIL has a better response to external forcing than that of CAM2. These indicate that the improvement of the dynamic core is very important. It is also verified that there is less predictability in the middle and high latitudes than in the low latitudes.

Key words: interannual variability, circulation, ensemble, GAMIL, CAM2

DOI: 10.1007/s00376-007-0082-1

1. Introduction

To get a confidential prediction for future climate evolution, it is necessary to validate the capability of numerical models in reproducing the observed climate variability. Due to the non-linear and chaotic behaviour of the climate system, this can be done in a probabilistic manner. It is commonly agreed that the ensemble approach can reduce the internal variability of models and validate their capability in reproducing the observed climate variability. Now the ensemble approach has been widely used in the literature (Harzallah and Sadourny, 1995; Wang and Rui, 1996; Li, 1999; Koster and Suarez, 2003; Nakaegawa et al., 2004; Wang and Guo, 2004) to study the atmospheric response to external anomalies.

By the ensemble approach, the total variability can be divided into two parts: an internal part due to atmospheric dynamics and an external part due to the external forcing variability. It is shown that the model internal variability is larger than the external variability except for the equatorial strip (Li, 1999), which indicates that the potential predictability is best in the low latitude regions and decreases with the latitude. As a matter of fact, Nakaegawa et al. (2004) and Derome et al. (2005) pointed out that a large part of the predictable component of the variability probably comes from some atmospheric forcing by the lower boundary, such as sea surface temperature, sea ice, or soil anomalies. The atmospheric process is more complicated in the mid-high latitudes and there is less predictability than in the low latitudes. This paper will provide further evidence for this conclusion by applying the analysis of variance approach to an ensemble experiment of a new AGCM recently developed at the Institute of Atmospheric Physics (IAP), Chinese Academy of Sciences (CAS), which is incorporated with the physical packages from the Community

*E-mail: yjl@mail.iap.ac.cn

Atmospheric Model Version 2 (CAM2) of the National Center for Atmospheric Research (Collins et al., 2003).

Because the two large-scale climate models have the same physical processes, it is meaningful to assess their simulation performances. This paper focuses on comparing the two models' circulation simulation performances of interannual variability for its important role in climate variability simulation. Section 2 introduces our experiment design and data. Section 3 presents the results of this experiment. The two models' performances are compared in the following aspects: total space-time variability simulation, Southern Oscillation Index (SOI) simulation, the responses of model internal variability to external forcing anomalies with the approach of variance analysis, Empirical Orthogonal Function (EOF) analysis to study interannual variability of the Northern Hemisphere winter 500-hPa geopotential height field, and two winter circulation indexes to study the East Asia simulation. The significance of the ensemble approach is also discussed during the experiment. Section 4 concludes the study.

2. Experiment design and data

2.1 *Model and experiment design*

As mentioned above, the two models have different dynamical cores, but the same physical processes. They both consist of an atmospheric component, a simple Sea Ice Component and a land process. The full name of the model used here is GAMIL1.0 (Gridpoint Atmospheric Model of IAP LASG). Its dynamical core includes a fully discrete finite difference approach with exact quadratic conservations, and a two-step shape-preserving advection scheme. Horizontally, the T42 Gaussian grid is used between 65.58°N and 65.58°S, and a weighted equal-area grid is used elsewhere. Vertically, there are 26 σ-coordinate layers, with the model top situated on an isobaric surface of 2.194 hPa. Details can be found in Wang et al. (2004).

In this experiment, the number of horizontal grid points adopted is 60×128 for GAMIL and 64×128 for CAM2, and the vertical resolution for each model is 26 levels. The ensemble approach is used to evaluate the two model's interannual variability performances objectively. The initial condition for each simulation is chosen randomly from 1 January of different years from respective Atmospheric Model Intercomparison Project (AMIP) control runs performed with climatological Sea Surface Temperature and Sea Ice Concentration boundary conditions, but the periods of the AMIP control runs are identical for the corresponding simulation for the two models. The ensemble members for each model are eight in number.

2.2 *Data*

The solar constant, orbital parameters and some gas concentrations are appointed according to the AMIP II protocol. With the AMIP II proposed approach, SST and SIC boundary conditions are obtained based on ERA-40 monthly mean SST and SIC observation data. Details for the approach can be found in Taylor et al. (2000).

The observed data for comparison are NCEP/DOE AMIP-II Reanalysis data (Kanamitsu et al., 2002) and CPC Merged Analysis of Precipitation data (Xie and Arkin, 1997). The horizontal resolution of geopotential height, sea level pressure and precipitation is 2.5°×2.5°, and the resolution of the 2-meter temperature is a T62 Gaussian grid (the number of horizontal grid points is 192×94).

In order to be compared in an identical manner, the output data of CAM2 and observed data are first interpolated to GAMIL grids. Eight simulations of each model are averaged before comparison. The integral periods of January 1979 to February 2003 are analyzed in this paper.

3. Results

3.1 *Total space-time variability analysis*

Taylor (2001) devised a diagram that can provide a concise statistical summary of how well patterns match each other in terms of their (simulation and observation, here) correlation, their root-mean-square difference, and the ratio of their variances. It is especially useful in evaluating complex models,such as those used to study geophysical phenomena. So the two models' simulation performances are evaluated with a total space-time Taylor diagram firstly. The analyzed fields are: 500-hPa geopotential height (Z500), precipitation (P), sea level pressure (PSL), and 2-meter temperature (T2M). The statistics presented in Fig. 1 are the simulated standard deviation (proportional to the radial distance) and correlation (related to the azimuthal angle) with observations of the total spatial and temporal variability (including the seasonal cycle, but subtracting the global mean, according to IPCC (2001). The simulated standard deviation has been normalized by the observed standard deviation. The statistics are for seasonal data (There are 97 seasons for January 1979 to February 2003), and they are weighted by the area of each grid cell. It is shown that both models can well simulate the 500-hPa geopotential height and 2-meter temperature, with a standard deviation very close to the observed one, and a correlation coefficient above 0.95. The performance for precipitation is less satisfying with a smaller standard deviation and a smaller

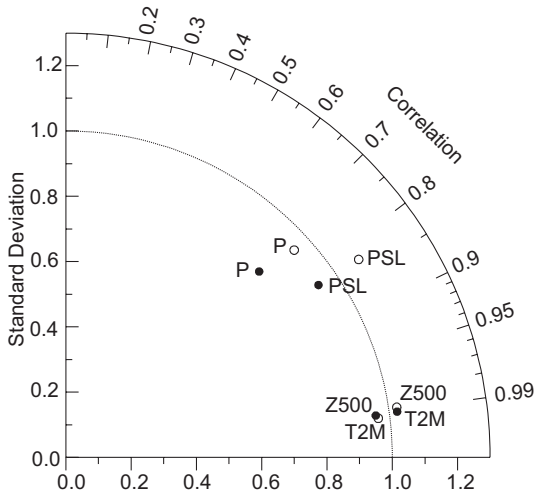

Fig. 1. The total space-time Taylor diagram for the two models (open circles for CAM2, closed circles for GAMIL). The analyzed fields are: 500-hPa geopotential height (Z500), precipitation (P), sea level pressure (PSL), and 2-meter temperature (T2M). The statistics shown are the standard deviation (proportional to the radial distance) and correlation (related to the azimuthal angle) with observations of the total spatial and temporal variability. The simulated standard deviation has been normalized by the observed standard deviation.

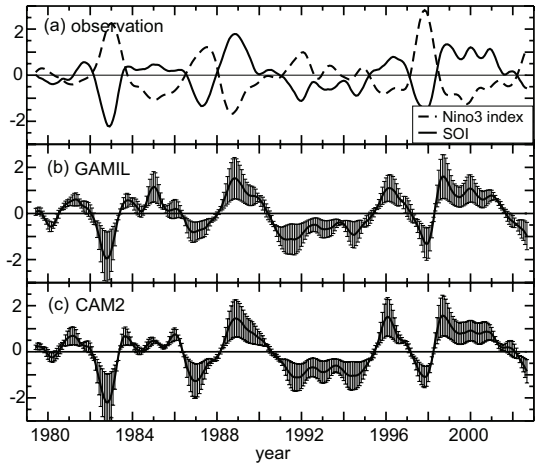

Fig. 2. Time series for (a) observed Niño-3 index (unit: K) and Southern Oscillation Index; (b) the simulated SOI of GAMIL; (c) the simulated SOI of CAM2. The x-axis is the year, and the y-axes are the SST anomaly for the Niño-3 index and the Standard Deviation for SOI.

correlation coefficient (0.7). These conclusions are similar to the PCMDI Report (Gates et al., 1999), and indicate that GAMIL has a comparative simulation performance to CAM2 on total space-time variability.

The total space-time variability for each simulation of the two models is also studied (figure not shown here), and it is found that the ensemble mean does have a reduced variance and a better temporal correlation to the observations, but the difference is inconspicuous. This conclusion coincides with Taylor (2001), who analyzed the normalized statistics for rainfall over India computed between pairs of simulations comprising one model's six-member ensemble and found that the correlation between pairs of realizations is very high. He figured out that the monthly mean climatology of rainfall over India is largely determined by the imposed boundary conditions (i.e., insolation pattern, sea surface temperatures, etc.) according to this model (run under AMIP experimental conditions) and that noise resulting from internal variations is relatively small. As we know, the ensemble approach is expected to reduce the internal model variations. However, both Taylor's conclusion and our study indicate that the ensemble mean may have little significance for a single model to study the total spatial and temporal variability simulation performance.

3.2 *Southern Oscillation Index simulation*

The southern Oscillation is an important interannual variability phenomenon. The formula that the NCEP Climate Prediction Center (CPC) uses to calculate the SOI is expressed as:

$$\mathrm{SOI(month,\ year)}=\frac{T(\mathrm{month,\ year})-D(\mathrm{month,\ year})}{S}\,, \tag{1}$$

where T and D are anomalies of the Tahiti (17.5°S, 149.6°W) and Darwin (12.4°S, 130.9°E) station sea level pressure that have been normalized by the standard deviation of the monthly values of the respective index for all months combined for January 1979 to February 2003, and S is the standard deviation of the numerator for all months combined for the same period. Firstly, the observed (here, the NCEP/DOE AMIP-II Reanalysis data) and simulated monthly mean sea level pressure is interpolated to the Tahiti and Darwin stations before calculating the indexes. The time series of all variables in Fig. 2 are filtered with a low-pass 11-term filter to eliminate high frequency signals and retain the interannual variability trend according to Trenberth (1984). Figure 2a is the observed Niño-3 SST and SOI, which are anti-phasic. Figures 2b and 2c are the simulated SOI of GAMIL and CAM2. The error bars are the standard deviation calculated from the eight ensemble members of each model. Both models can simulate the interannul var-

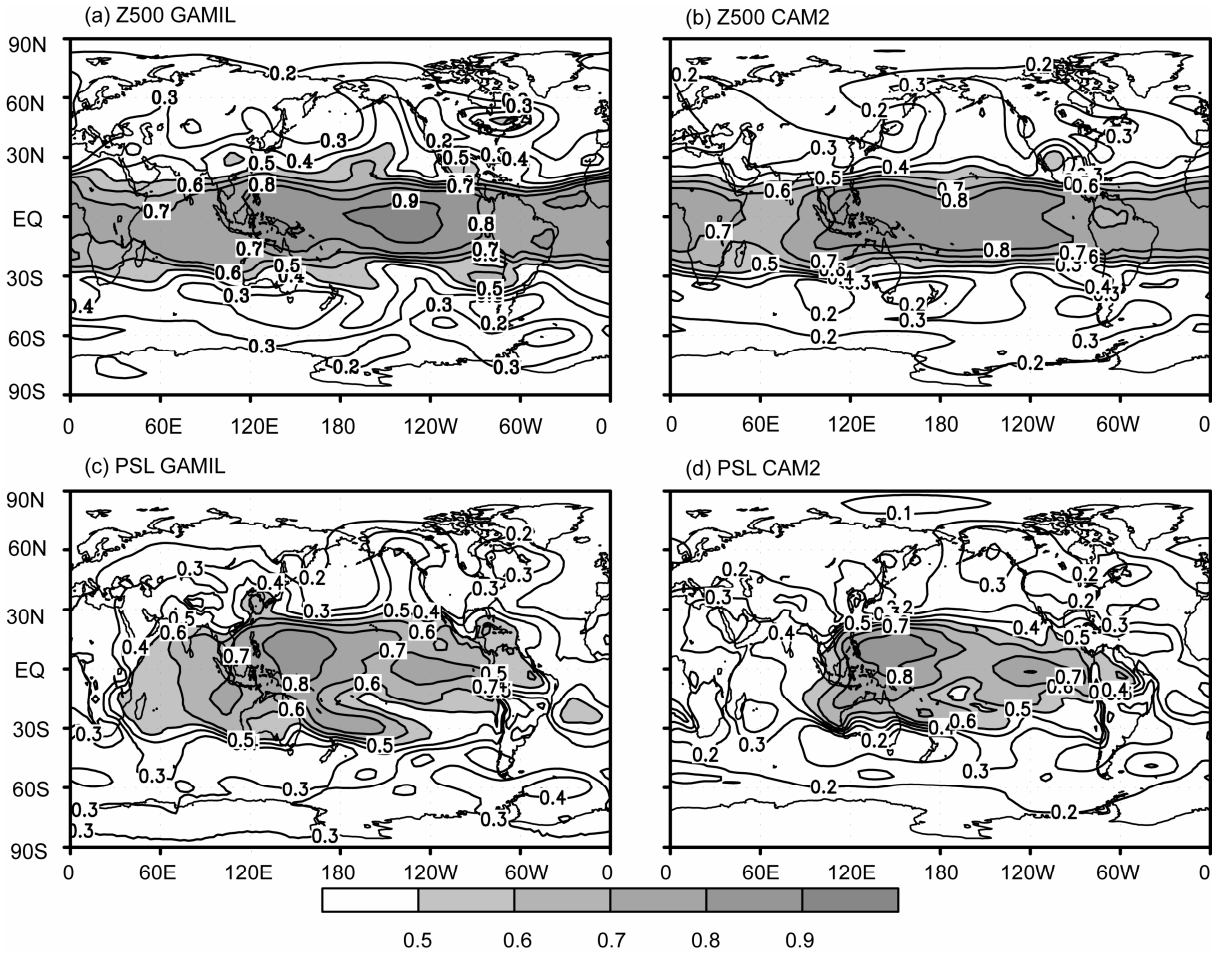

Fig. 3. The signal to noise ratios of winter 500-hPa geopotential height (Z500) and sea level pressure (PSL) fields for GAMIL [(a) and(c)] and CAM2 [(b) and (d)].

ia bility well with a time correlation coefficient near 0.9, which is statistically significant at the 99% confidence level (a t-test is used in this paper), and indicates that the two models have similar SOI simulation performance. It is interesting that the standard deviation is bigger when the curve reaches its extremum, while the standard deviation is close to zero when the curve reaches its zero value. This may indicate that the scatter degree of the simulations is bigger during the period of an El Niño event and that the ensemble mean still retains its significance even in the low latitudes.

3.3 *External forcing versus internal variability*

From the point of view of climate prediction, the atmospheric response to SST forcing can be considered as climatic noise and climatic signal. Therefore the total climate variability can be divided into external variability and internal variability. Many works in the literature apply the approach of variance analysis to study the response of the internal atmospheric dynamics to external forcing variability (such as Zwiers, 1996; Wang and Rui, 1996; and Li, 1999). This approach uses the signal to noise ratio, and it is applied to the internal variability of the winter 500-hPa geopotential height and sea level pressure fields. The decomposition is performed with the following equations:

$$x_{\mathrm{e}}(y) = \frac{1}{N}\sum_{n=1}^{N} x(n,y)\,, \tag{2}$$

$$x_{\mathrm{c}} = \frac{1}{NY}\sum_{n=1}^{N}\sum_{y=1}^{Y} x(n,y) = \frac{1}{Y}\sum_{y=1}^{Y} x_{\mathrm{e}}(y)\,, \tag{3}$$

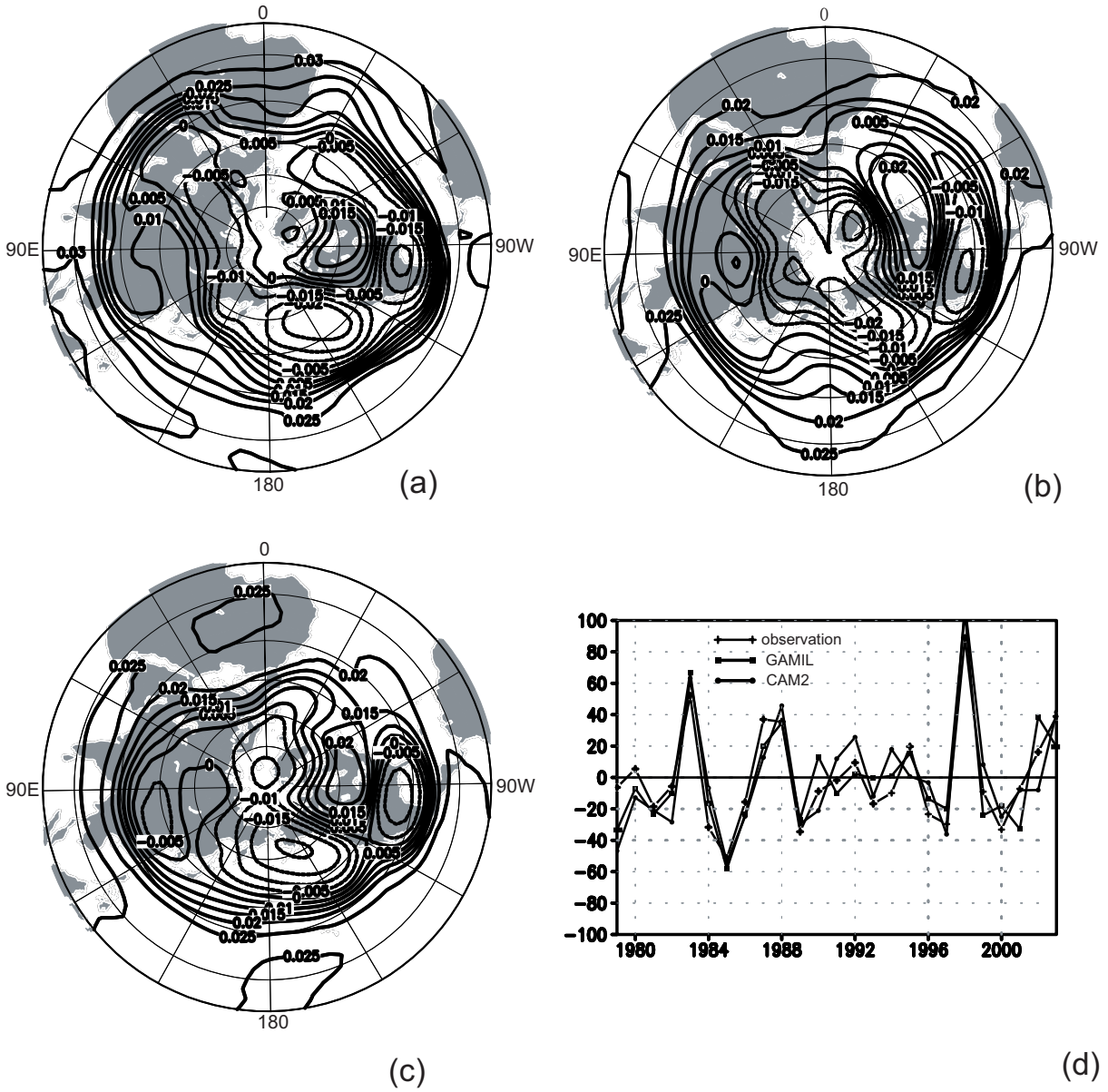

Fig. 4. The leading EOF structure of Northern Hemisphere winter 500-hPa geopotential height for (a) the observations, (b) GAMIL and (c) CAM2; (d) are the expanded time coefficients for the first mode.

$$\sigma_{\rm i}^2 = \frac{1}{Y}\sum_{y=1}^{N}\left\{\frac{1}{N}\sum_{n=1}^{N}[x(n,y)-x_{\rm e}(y)]^2\right\}\,, \quad (4)$$

$$\sigma_{\rm e}^2 = \frac{1}{Y}\sum_{y=1}^{Y}[(x_{\rm e}(y)-x_{\rm c}]^2\,, \quad (5)$$

$$\sigma_{\rm t}^2 = \sigma_{\rm e}^2 + \sigma_{\rm i}^2\,, \quad (6)$$

$$\lambda = \sigma_{\rm e}^2/\sigma_{\rm t}^2\,, \quad (7)$$

where x is a time series of a monthly mean (or seasonal mean) variable, and $x(n,y)$ is the value of the nth simulation sample in an ensemble of size N for the yth year of a simulation of length Y. $x_{\rm e}$ is the ensemble mean and $x_{\rm c}$ is the climatological mean. $\sigma_{\rm e}^2$, $\sigma_{\rm i}^2$ and $\sigma_{\rm t}^2$ are external variance, internal variance and total variance. λ is defined as the signal to noise ratio. The bigger λ is, the smaller the model internal noise is relative to the external signal, and the better potential predictability the model has. Figure 3 plots the signal to noise ratio for the winter 500-hPa geopotential height and sea level pressure fields. Generally speaking, both models have good potential predictability performance in the equatorial regions with λ around

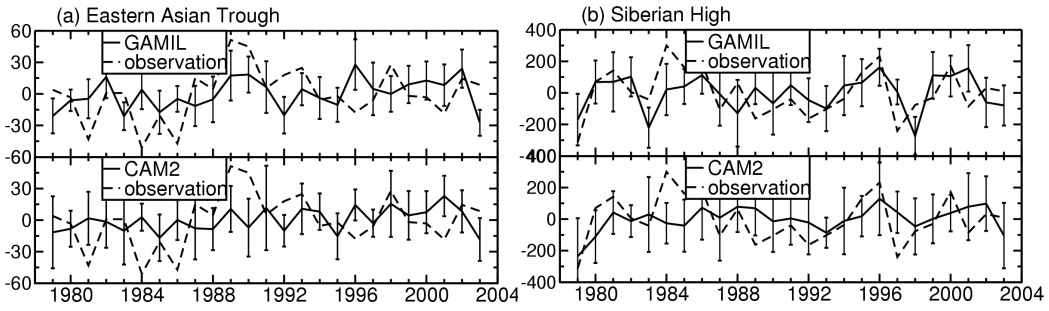

Fig. 5. Observed and simulated winter Northern Hemisphere circulation indexes: (a) East Asian Trough (unit: gpm), (b) Siberian High (unit: Pa). The solid lines are simulated, the dashed are observed.

0.8–0.9. λ decreases to about 0.2 in the high latitudes. It seems that GAMIL has a better predictability performance than CAM2 in the equatorial strip and subtropical regions. It is also revealed that, for both models, the 500-hPa geopotential height field has a better predictability performance than the sea level pressure field.

3.4 *Winter Northern Hemisphere and East Asian circulation analysis*

Finally, the interannual simulation performances of the winter Northern Hemisphere and East Asia are analyzed. It is known that different data pretreatments may result in different Empirical Orthogonal Function (EOF) mode patterns (Wei, 1999). The winter (DJF) data (ensemble mean for each model) used are normalized before EOF analysis. Figure 4 shows the leading EOF modes and the expanded time coefficients for the observed and simulated 500-hPa geopotential height fields. We can see from Fig. 4a that the first mode is a Pacific North American (PNA) pattern. The explained variance by the leading EOF is 25% in the observations, 30% in GAMIL, and 33% in CAM2. The spatial correlation coefficient of the leading EOF is 0.80 between the observations and GAMIL, and 0.82 between the observations and CAM2. The correlation coefficient of the leading expanded time coefficients is 0.90 between the observations and GAMIL, and 0.87 between the observations and CAM2. It is obvious that the two models have close leading EOF space and expanded time coefficients with the observations, which indicates that both the models can capture the principal characteristics of the observations. Similar to the result in Li (1999), the simulated Pacific North American pattern is shifted westward in the first mode, which indicates that the simulated convection activity response to the warm episode of El Niño is too weak over the eastern part of the tropical Pacific.

The simulation of the East Asian circulation is also a basic aspect in examining a model's performance. Here the two models' simulation performance of two winter interannual variability circulation indexes are compared, namely the East Asian Trough (30°–50°N, 120°–150°E) in the 500-hPa geopotential height field and the Siberian High (40°–60°N, 70°–120°E) in the sea level pressure field. The circulation indexes the are defined as area mean anomaly of the year-by-year winter mean (DJF) data according to Liu et al. (2004). The correlation coefficient is 0.45 between GAMIL and the observations, and 0.37 between CAM2 and the observations for the Siberian High, and the correlation coefficient is 0.14 between GAMIL and the observations, and 0.0002 between CAM2 and the observations for the East Asian Trough. It is found that both models simulate the Siberian High well and pass the statistical significance test at the 95% confidence level (t-test), while neither model simulates the East Asian Trough well nor passes statistical significance. And it is also indicated that GAMIL simulates the two circulation indexes a little better than CAM2, which might prove that GAMIL can simulate the East Asia region better. Figure 5 shows that the simulated indexes deviate by more or less than a standard deviation, which indicates that the greater the standard deviation is, the more significant the ensemble mean is.

4. Conclusions

This paper focuses on assessing the interannual variability circulation simulation performances of two models with the same physical processes using the ensemble approach. GAMIL has comparative performances with CAM2 on total space-time variability and SOI simulation. It verifies that both models have good reproducibility performance in the equatorial regions, but poor performance in higher latitudes. GAMIL has a better predictability performance than CAM2 in the equatorial strip and extra-tropical region. In an EOF analysis of the winter Northern Hemisphere 500-hPa geopotential height field, it is found that the two mod-

els can capture well the principal features of the observations, but they show different correlations to the observations due to different variances. GAMIL simulates the winter East Asian circulation indexes a little better than CAM2, which might indicate that GAMIL can simulate the East Asia region better.

In a word, the two models have similar interannual variability simulation performances, and GAMIL simulates the East Asian winter circulation better than CAM2. These conclusions validate that the improvement of the dynamical core is significant.

Acknowledgements. This paper was supported by the Science Funds for Creative Research Groups (Grant No. 40221503) and the 973 Project (Grant No. 2005CB321703). All simulations were conducted on a Deepcomp 6800 computer at the Super Computing Center, Computer Network Information Center, Chinese Academy of Sciences.

REFERENCES

Collins, W. D., and Coauthors, 2003: *Description of the NCAR Community Atmosphere Model (CAM2).* NCAR Tech. Note, 171pp.

Derome, J., H. Lin and G. Brunet, 2005: Seasonal forecasting with a simple general circulation model: Predictive Skill in the AO and PNA. *J. Climate,* **18**, 597–609.

Gates, W. L., and Coauthors, 1999: An overview of the results of the Atmospheric Model Intercomparison Project (AMIP I). *Bull. Amer. Meteor. Soc.*, **80**, 29–55.

Harzallah, A., and R. Sadourny, 1995: Internal versus SST-forced atmospheric variability as simulated by an atmospheric general circulation model. *J. Climate*, **8**, 474–495.

IPCC, 2001: *Climate Change 2001, The Scientific Basis. Contribution of working Group I to the Third Assessment Report of the Inter-governmental Panel on Climate Change* (*IPCC*), Houghton et al., Eds., Cambridge University Press, 892pp.

Kanamitsu, M., W. Ebisuzaki, J. Woollen, S.-K. Yang, J. J. Hnilo, M. Fiorino, and G. L. Potter, 2002: NCEP-DEO AMIP-II Reanalysis (R-2). *Bull. Amer. Meteor. Soc.*, **83**, 1631–1643.

Koster, R. D., and M. J. Suarez, 2003: Impact of land surface initialization on seasonal precipitation and temperature prediction. *Journal of Hydrometeorology*, **4**, 408–423.

Li, Z. X., 1999: Ensemble atmospheric GCM simulation of climate interannual variability from 1979 to 1994. *J. Climate*, **12**, 986–1001.

Liu Yanxiang, Ma Xiaoyan, and Guo Yufu, 2004: Outer forcing influence on winter Northern Hemisphere circulation simulation in decadal variability. *Plateau Meteorology,* **23**(4), 458–464. (in Chinese)

Nakaegawa, T., M. Kanamitsu, and T. M. Smith, 2004: Interdecadal trend of prediction skill in an ensemble AMIP-type experiment. *J. Climate*, **17**, 2881–2889.

Taylor, K. E., 2001: Summarizing multiple aspects of model performance in a single diagram. *J. Geophy. Res.*, **106**(D7), 7183–7192.

Taylor, K. E., D. Williamson, and F. Zwiers, 2000**:** *The sea surface temperature and sea-ice concentration boundary condition for AMIP II simulations.* PCMDI Report No.60, Program for Climate Model Diagnosis and Intercomparison, Lawrence Livermore National Laboratory, Livermore, CA, 25pp.

Trenberth, K. E., 1984: Signal versus noise in the Southern Oscillation. *Mon. Wea. Rev.*, **112**, 326–321.

Wang Bin, Wan Hui, Ji Zhongzhen, Zhang Xin, Yu Rucong, Yu Yongqiang, and Liu Hailong, 2004: Design of a new dynamical core for global atmospheric models base on some efficient numerical methods. *Science in China*(A), **47**, 4–21.

Wang Jia, and Guo Yufu, 2004: Possible impacts of Barents sea ice on the Eurasian atmospheric circulation and the rainfall of East China in the beginning of summer. *Adv. Atmos. Sci.*, **21**(4), 662–674.

Wang, X. L, and H. L. Rui, 1996: A methodology for assessing ensemble experiments. *J. Geophys. Res.*, **101D**, 29591–29597.

Wei Fengying, 1999: *Modern Climate Diagnose and Forecast Technique.* China Meteorology Press, Beijing, 269pp. (in Chinese)

Xie, P., and P. A. Arkin, 1997: Global precipitation: A 17-year monthly analysis based on gauge observations, satellite estimates, and numerical model outputs, *Bull. Amer. Meteor. Soc.*, **78**, 2539–2558.

Zwiers, F. W., 1996: Interannual variability and predictability in an ensemble of AMIP climate simulations conducted with the CCC GCM2. *Climate Dyn.*, **12**, 825–847.